Resonance v Osončju

Resonanca
1 : 2

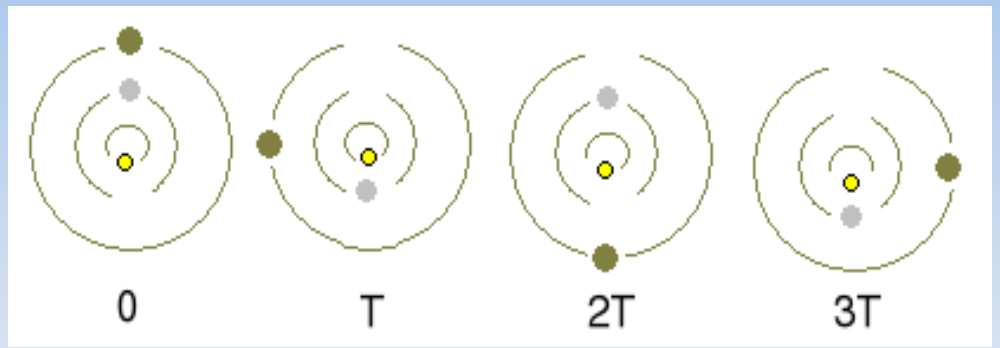

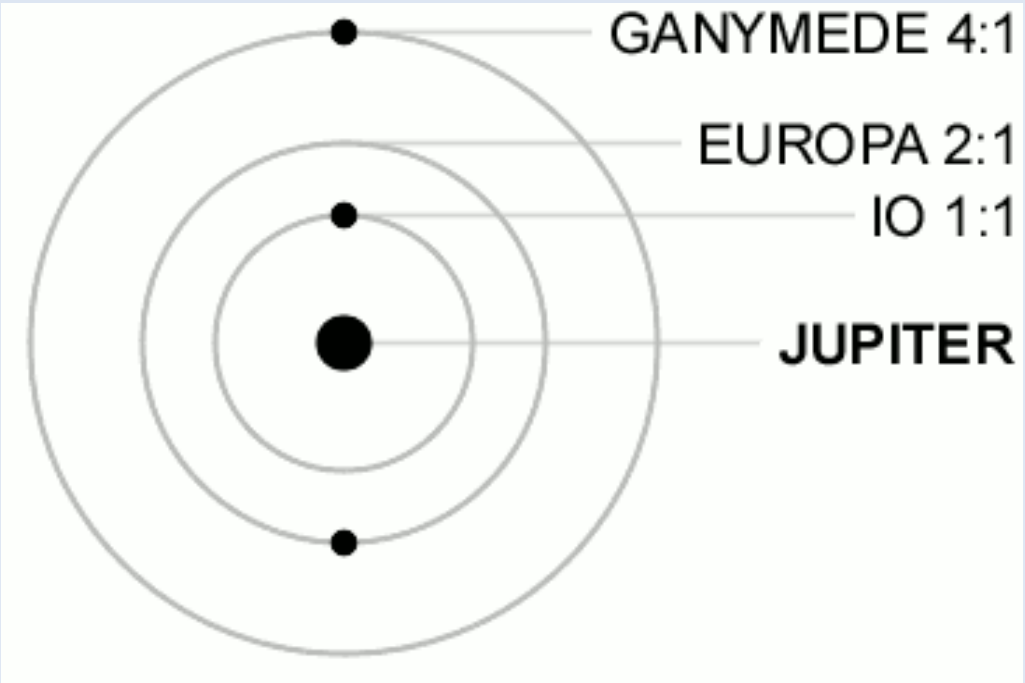

Druge orbitalne resonance:
- 2:3 Pluto–Neptune
- 2:4 Tethys–Mimas (Saturnovi luni)
- 1:2 Dione–Enceladus (Saturnovi luni)
- 3:4 Hyperion–Titan (Saturnovi luni)
- 1:2:4 Ganymede–Europa–Io (Jupitrove lune)

vrzeli v asteroidnem pasu, Trojanci, Saturnovi obroči.

Resonance: Saturnovi obroči

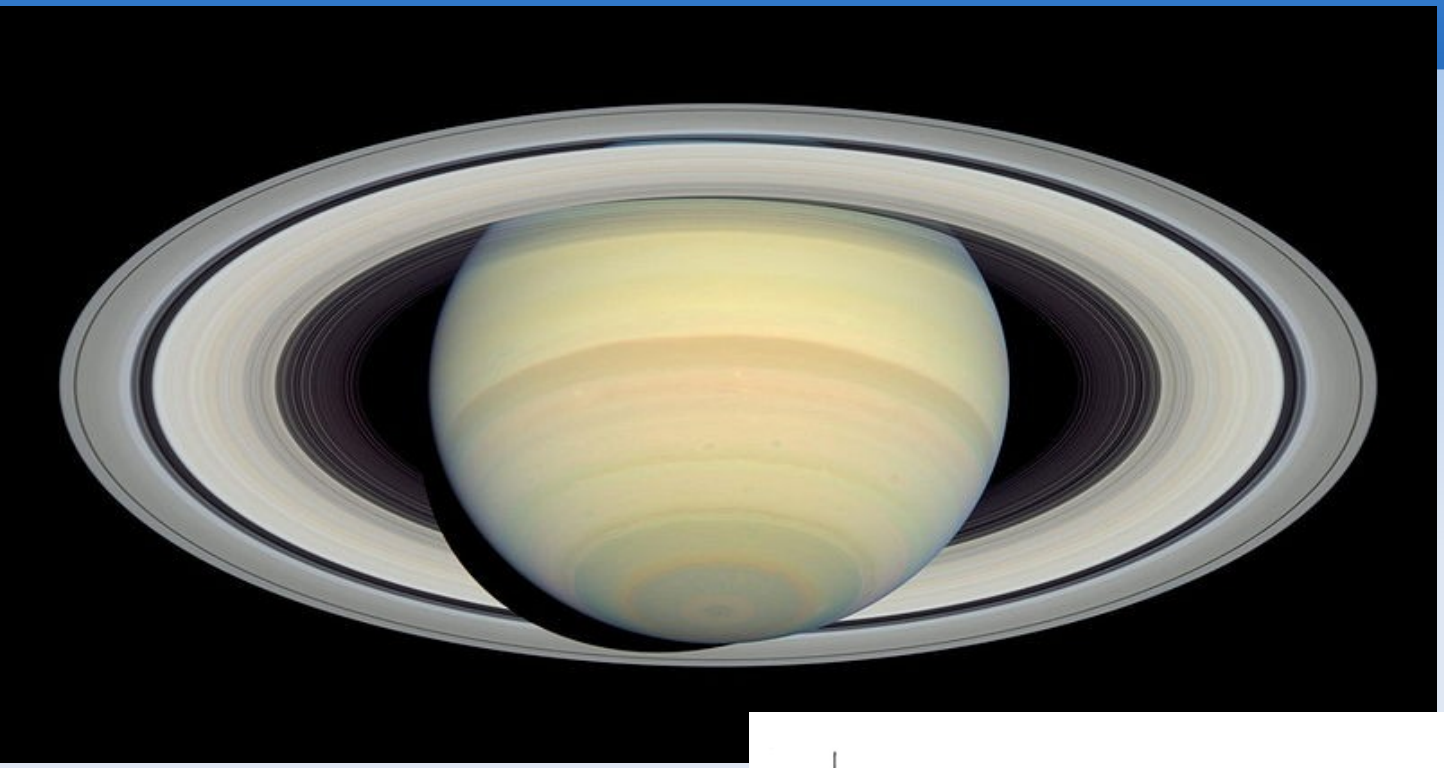

Resonanca 1:2
z luno Mimas.

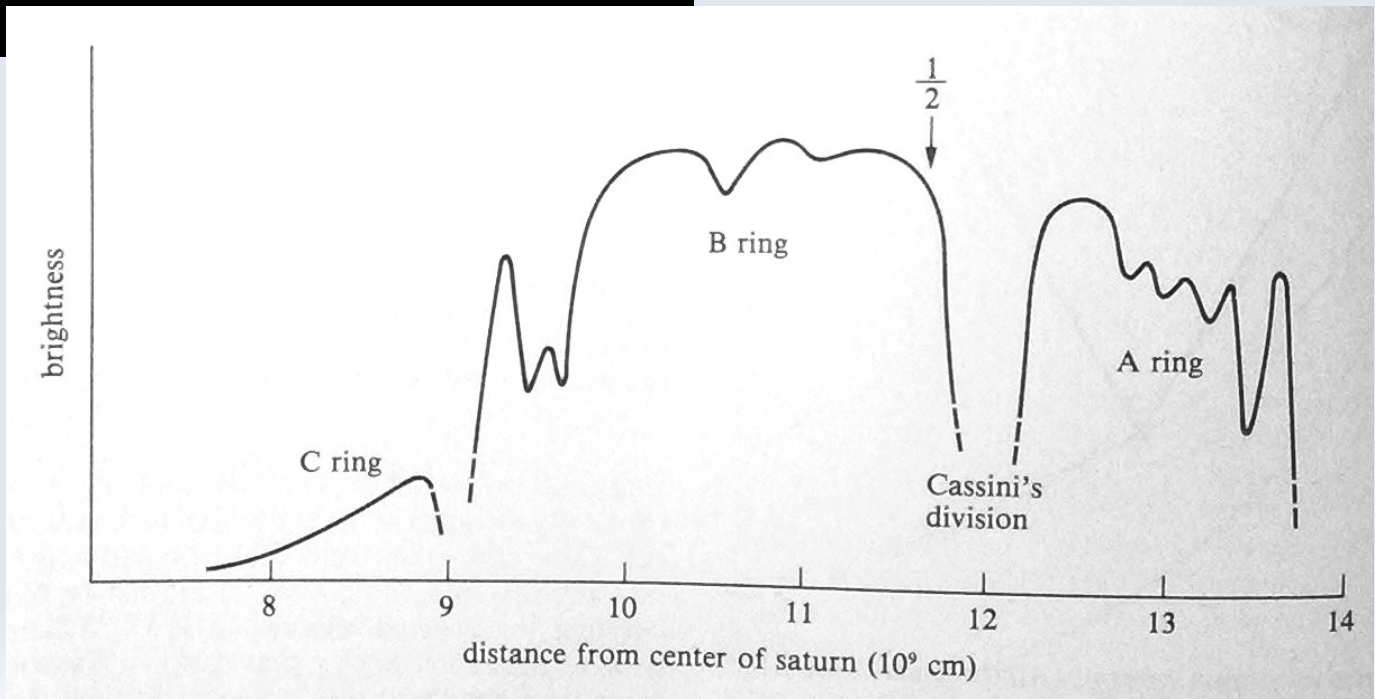

Resonance: Saturnovi obroči

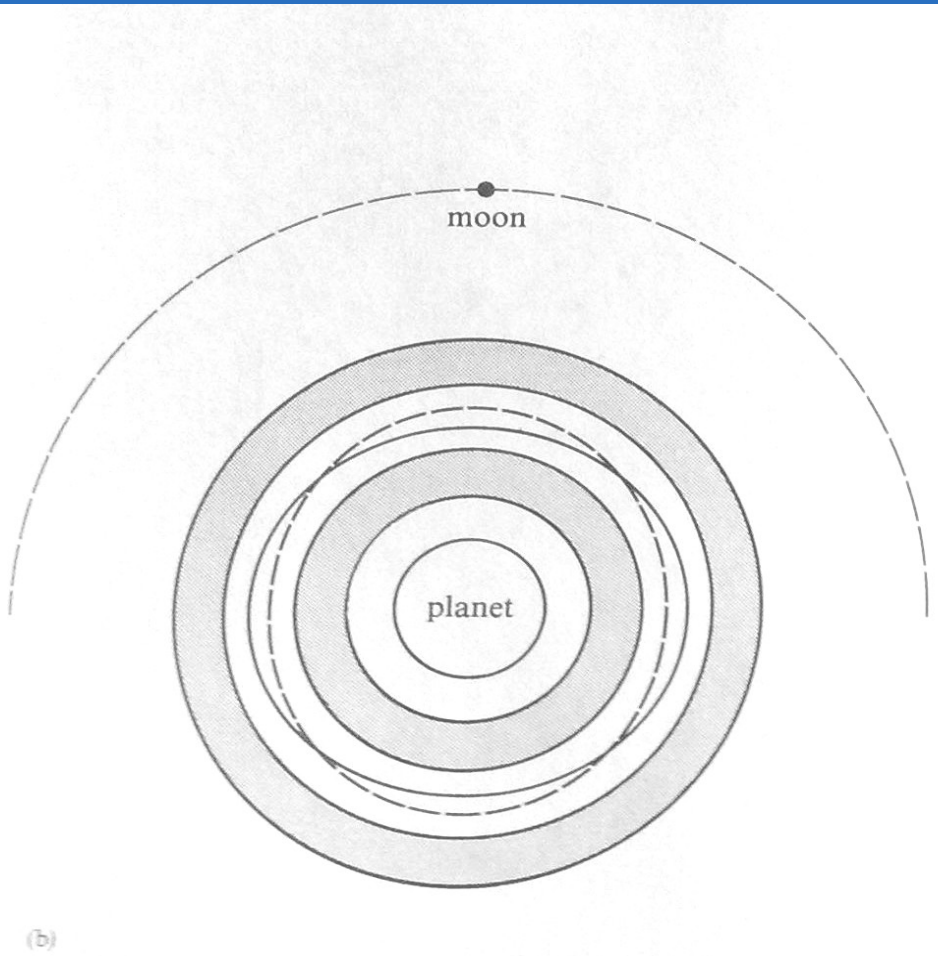

(b)

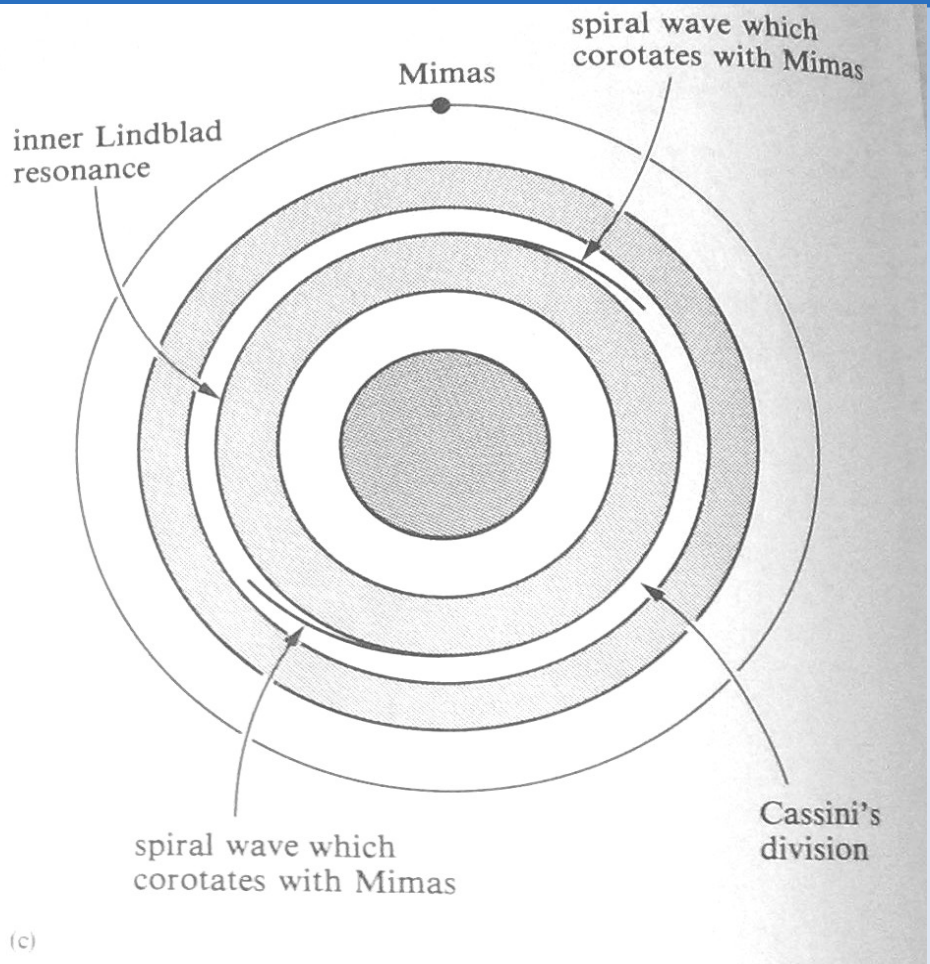

(c)

Figure 18.9. (b) The collisional mechanism for creating gaps at the locations of resonances associated with outer moons has been found inadequate to explain the prominent Cassini division. (c) Resonantly driven density waves have also been invoked to clear Cassini's division. Although this mechanism's ability to clear large gaps remains controversial, recent analysis has established that spiral density waves do exist in some parts of Saturn's rings.

F- Shu: The Physical Universe

Rochev potencial

privzamemo: krožna tira, točkasti masi

$$\Phi_R = - G M_1 / |r - r_1|^{-1} - G M_2 / |r - r_2|^{-1} - \tfrac{1}{2} (\omega \times r)^2$$

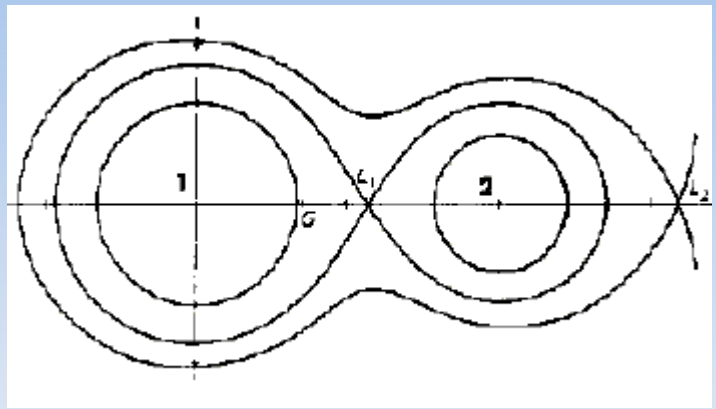

5 Lagrangeovih točk, v katerih je odvod potenciala nič.

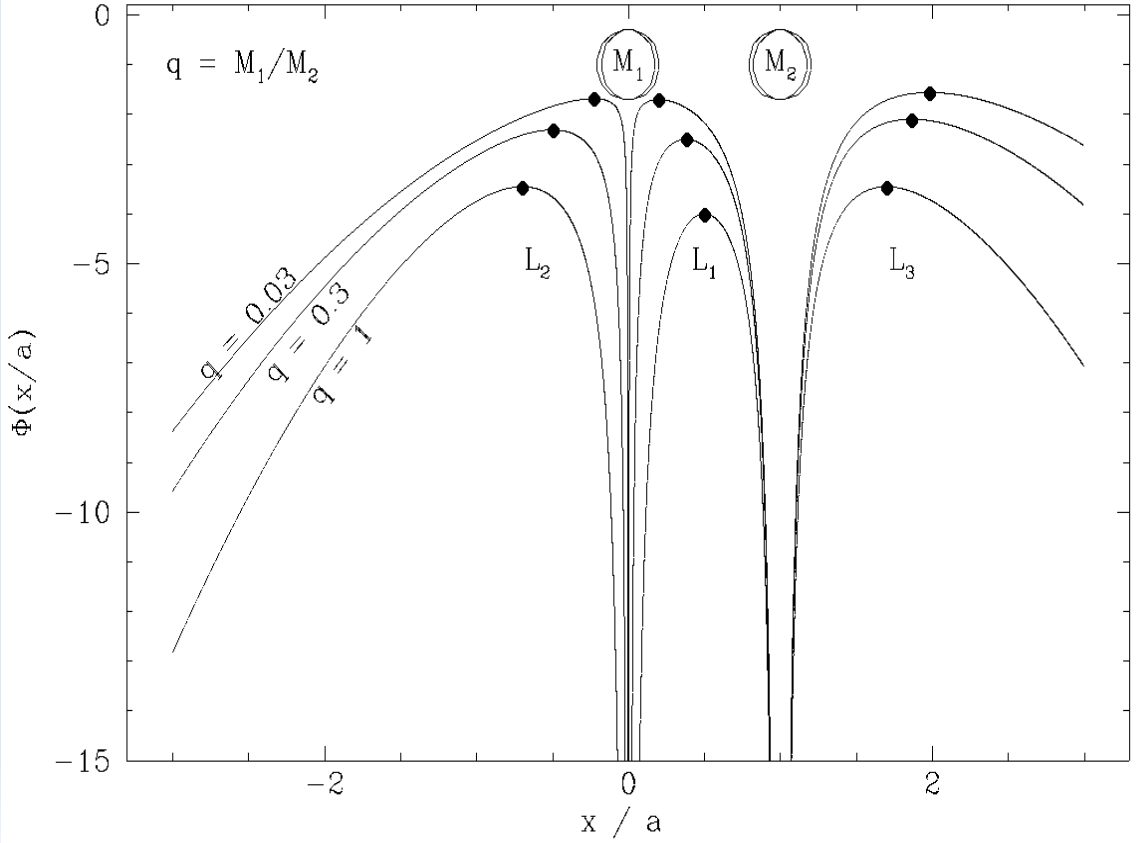

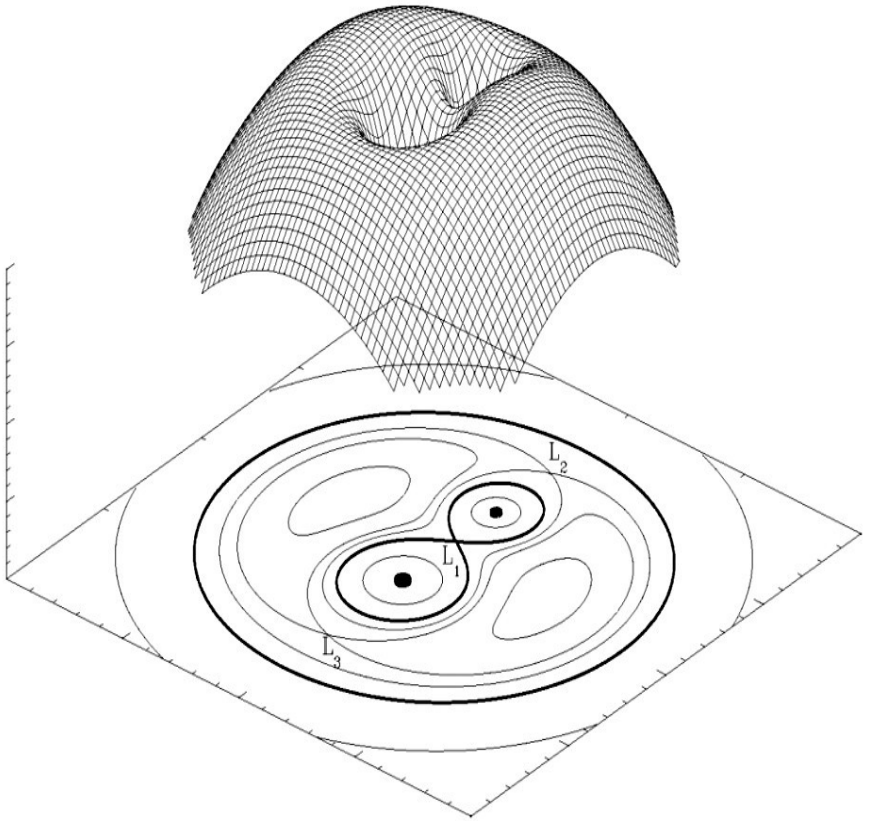

Rochev potencial

1. Distance R_{L_1} from centre of primary to inner Lagrangian point

$$\frac{R_{L_1}}{a} = 1 - w + \frac{1}{3}w^2 + \frac{1}{9}w^3 \qquad (2.4a)$$

where

$w^3 = \frac{q}{3(1+q)}$	$q \le 0.1$	Kopal (1959)	
$\frac{R_{L_1}}{a} = 0.500 - 0.227 \log q$	$0.1 \le q \le 10$	Plavec & Kratochvil (1964)	(2.4b)
$= (1.0015 + q^{0.4056})^{-1}$	$0.04 \le q \le 1$ error < 1%	Silber (1992)	(2.4c)

2. Volume radius $R_L(2)$ of the Roche lobe of the secondary

$\frac{R_L(2)}{a} = 0.38 + 0.20 \log q$	$0.3 < q < 20$ accurate to 2%	Paczynski (1971)	(2.5a)
$\frac{R_L(2)}{a} = 0.462\left(\frac{q}{1+q}\right)^{1/3}$	$0 < q < 0.3$ accurate to 2%	Paczynski (1971)	(2.5b)
$\frac{R_L(2)}{a} = \frac{0.49q^{2/3}}{0.6q^{2/3} + \ln(1+q^{1/3})}$	$0 < q < \infty$ accurate to better than 1%	Eggleton (1983)	(2.5c)

3. Equatorial Roche lobe radius (y direction) of the secondary

$\frac{R_L(\text{eq})}{a} = 0.378q^{-0.2084}$	$0.1 < q < 1$ accurate to 1% over $0.2 \le q \le 1$	Plavec & Kratochvil (1964)	(2.5d)

4. Volume radius $R_L(1)$ of the Roche lobe of the primary:
Put $q \to q^{-1}$ in equations (2.5a), (2.5b) or (2.5c), or use

$$\frac{R_L(1)}{a} = 0.396q^{-1/6} \qquad 0.07 \le q \le 0.6 \qquad (2.6)$$

which agrees with (2.5c) to within 2%.

$q = M_2 / M_1$

Resonance: asteroidi

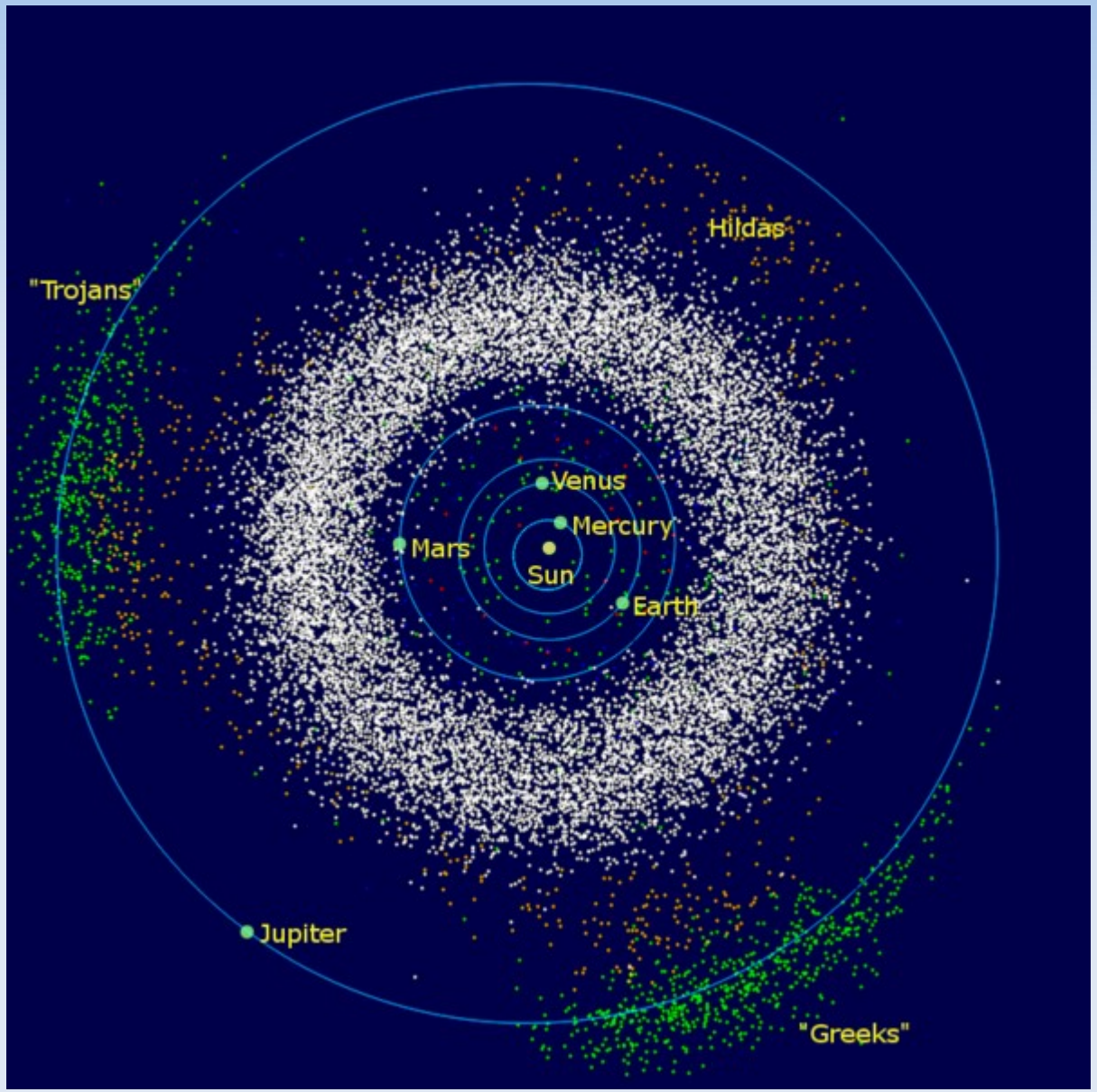

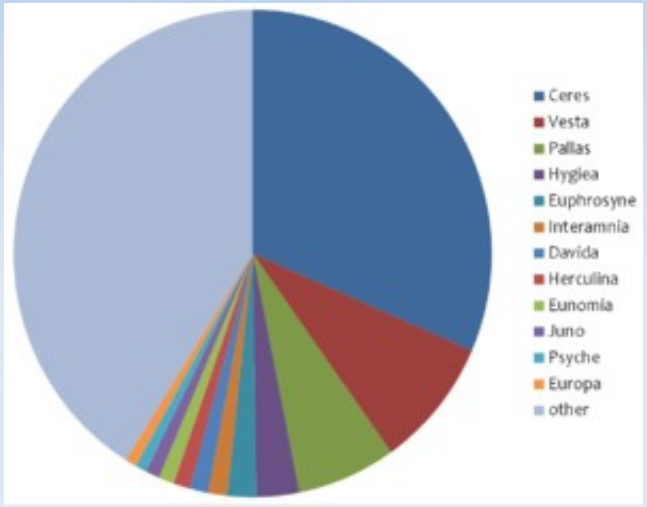

The relative masses of the twelve largest asteroids known,[36] compared to the remaining mass of the asteroid belt.[37]

Ceres	511 Davida
4 Vesta	532 Herculina
2 Pallas	15 Eunomia
10 Hygiea	3 Juno
31 Euphrosyne	16 Psyche
704 Interamnia	52 Europa
	all others

Resonance: asteroidi

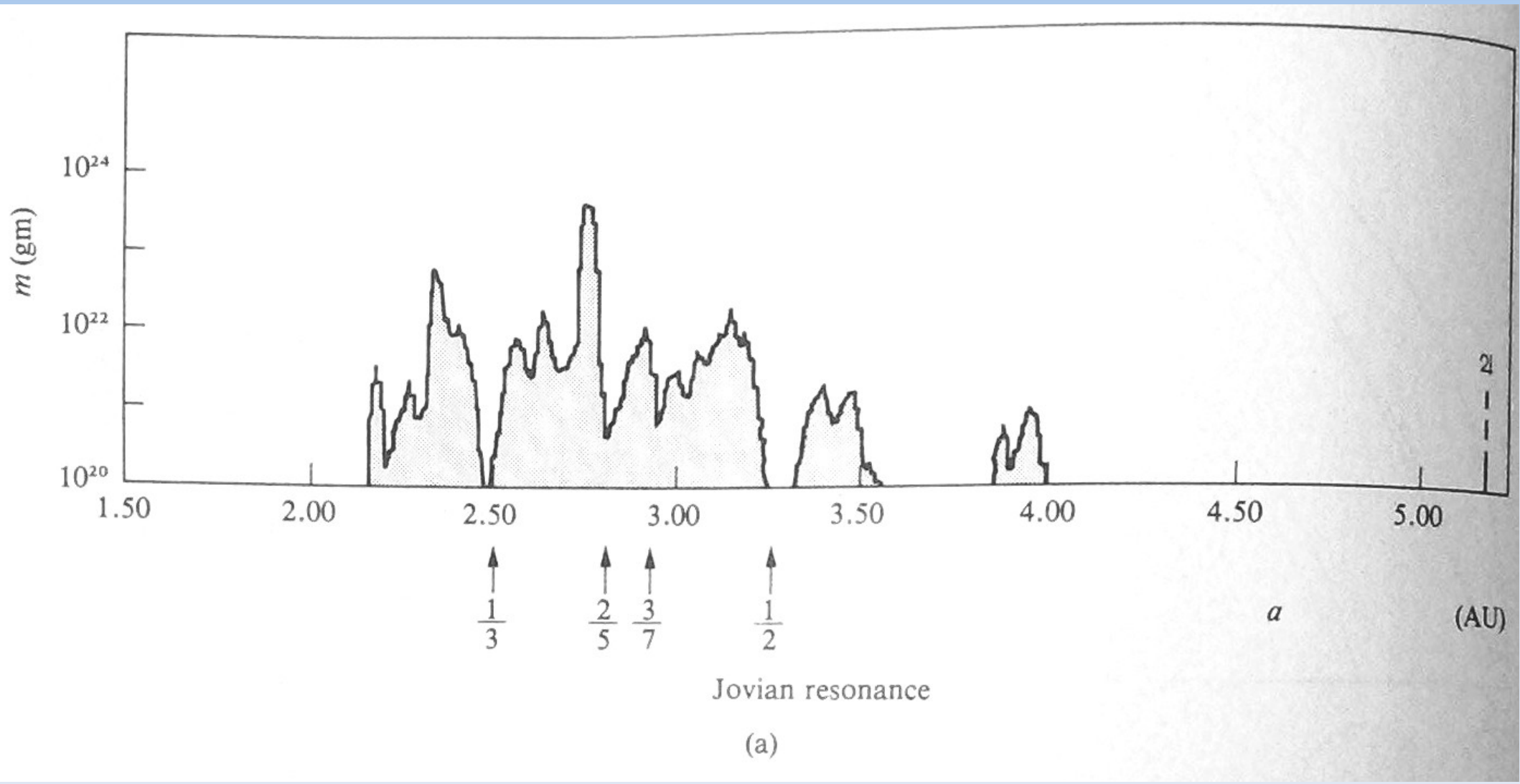

Spinske resonance

Luna: 1:1 (korotacija)
Merkur: 3:2 (3-krat se zavrti okoli lastne osi, ko pride 2-krat okoli Sonca)

Letters to Nature

Nature **429**, 848-850 (24 June 2004) | doi:10.1038/nature02609; Received 12 March 2004; Accepted 4 May 2004

Mercury's capture into the 3/2 spin-orbit resonance as a result of its chaotic dynamics

Alexandre C. M. Correia[1,2] & Jacques Laskar[2]

1. Departamento de Física da Universidade de Aveiro, Campus Universitário de Santiago, 3810-193 Aveiro, Portugal
2. Astronomie et Systèmes Dynamiques, IMCCE-CNRS UMR8028, Observatoire de Paris, 77 Avenue Denfert-Rochereau, 75014 Paris, France

Correspondence to: Jacques Laskar[2] Email: Laskar@imcce.fr

Mercury is locked into a 3/2 spin-orbit resonance where it rotates three times on its axis for every two orbits around the sun[1, 2, 3]. The stability of this equilibrium state is well established[4, 5, 6], but our understanding of how this state initially arose remains unsatisfactory. Unless one uses an unrealistic tidal model with constant torques (which cannot account for the observed damping of the libration of the planet) the computed probability of capture into 3/2 resonance is very low (about 7 per cent)[5]. This led to the proposal that core–mantle friction may have increased the capture probability, but such a process requires very specific values of the core viscosity[7, 8]. Here we show that the chaotic evolution of Mercury's orbit can drive its eccentricity beyond 0.325 during the planet's history, which very efficiently leads to its capture into the 3/2 resonance. In our numerical integrations of 1,000 orbits of Mercury over 4 Gyr, capture into the 3/2 spin-orbit resonant state was the most probable final outcome of the planet's evolution, occurring 55.4 per cent of the time.

Plimske sile

- **krožni tir**
- **mimolet**

(F. Shu: The Physical Universe, problem 14.2 in enačba 17.4.)

meteorski roji

Dejanske, skalirane, kotne velikosti

Name	#	Orbits	Distance (000 km)	O_Period (days)	Incl	Eccen	Discoverer	Date	A.K.A.
Sun	-	-	-	-	-	-	-	-	Sol (0)
Mercury	I	Sun	57910	87.97	7.00	0.21	-	-	(0)
Venus	II	Sun	108200	224.70	3.39	0.01	-	-	(0)
Earth	III	Sun	149600	365.26	0.00	0.02	-	-	(0)
Mars	IV	Sun	227940	686.98	1.85	0.09	-	-	(0)
Jupiter	V	Sun	778330	4332.71	1.31	0.05	-	-	(0)
Saturn	VI	Sun	1429400	10759.50	2.49	0.06	-	-	(0)
Uranus	VII	Sun	2870990	30685.00	0.77	0.05	Herschel	1781	(0)
Neptune	VIII	Sun	4504300	60190.00	1.77	0.01	Adams(9)	1846	(0)
Pluto	IX	Sun	5913520	90550	17.15	0.25	Tombaugh	1930	(0)
Moon	I	Earth	384	27.32	5.14	0.05	-	-	Luna (0)

Name	Radius (km)	Mass (kg)	Dens	Abo	Vo	Rotate (days)	Dimensions (km)
Sun	695000	1.99e30	1.41	?	-26.	24.6	
Mercury	2440	3.30e23	5.43	.11	-1.9	58.6	
Venus	6052	4.87e24	5.24	.65	-4.4	-243	
Earth	6378	5.97e24	5.52	.30	-	0.99	
Mars	3397	6.42e23	3.93	.15	-2.0	1.03	
Jupiter	71492	1.90e27	1.33	.52	-2.7	0.41	
Saturn	60268	5.68e26	0.69	.47	0.7	0.45	
Uranus	25559	8.68e25	1.32	.51	5.5	-0.72	
Neptune	24766	1.02e26	1.64	.41	7.8	0.67	
Pluto	1150	1.27e22	2.06	.55	13.6	-6.39	(z)
Moon	1738	7.35e22	3.34	.12	-12.7	S	

Name	Gravity (g)	Esc vel (km/s)	M.O.V (km/s)	Axial incl	Oblate	Ascend node	Peri-helion	Equilib (K)	Surface (K)	Press (atm)	Atmospheric Composition
Mercury	0.378	4.44	47.87	0		48.35	77.44	449	440	0	--
Venus	0.907	10.36	35.02	177.36		76.72	131.56	328	730	93	CO2, N2
Earth	1.000	11.19	29.79	23.45	.00335	354.90	102.83	279	287	1	N2, O2, Ar
Mars	0.377	5.03	24.13	25.19	.00519	49.60	335.99	226	218	0.007	CO2, N2, Ar
Jupiter	2.364	59.5	13.06	3.13	.06481	100.47	15.63	122	120	(x)	H2, He
Saturn	0.916	35.5	9.66	26.73	.1076	113.71	92.80	90	88		H2, He
Uranus	0.889	21.3	6.80	97.86	.030	74.06	176.29	64	59		H2, He, CH4
Neptune	1.125	23.5	5.44	29.60	.026	131.81	1.95	51	48		H2, He, CH4
Pluto	0.067	1.3	4.74	122.52		110.42	224.59	44	37	1e-5	N2, CH4, CO

Key:

Gravity	Equatorial surface gravity in g's (see also "Your Weight On Other Worlds")
Esc vel	Escape velocity in kilometers per second
M.O.V.	Mean Orbital Velocity in kilometers per second
Axial incl	Inclination of the rotation axis in degrees (obliquity)
Oblate	Oblateness
Ascend	Longitude of the ascending node
Perihelion	Longitude of perihelion
Equilib	Equilibrium temperature in Kelvins
Surface	Surface temperature in Kelvins
Press	Surface pressure in atmospheres

Notes:

(x) for the jovian planets "surface" refers to the cloud tops or 1 bar level

Much more accurate and detailed data is available from JPL's Horizons **telnet** interface

Meteorski roji

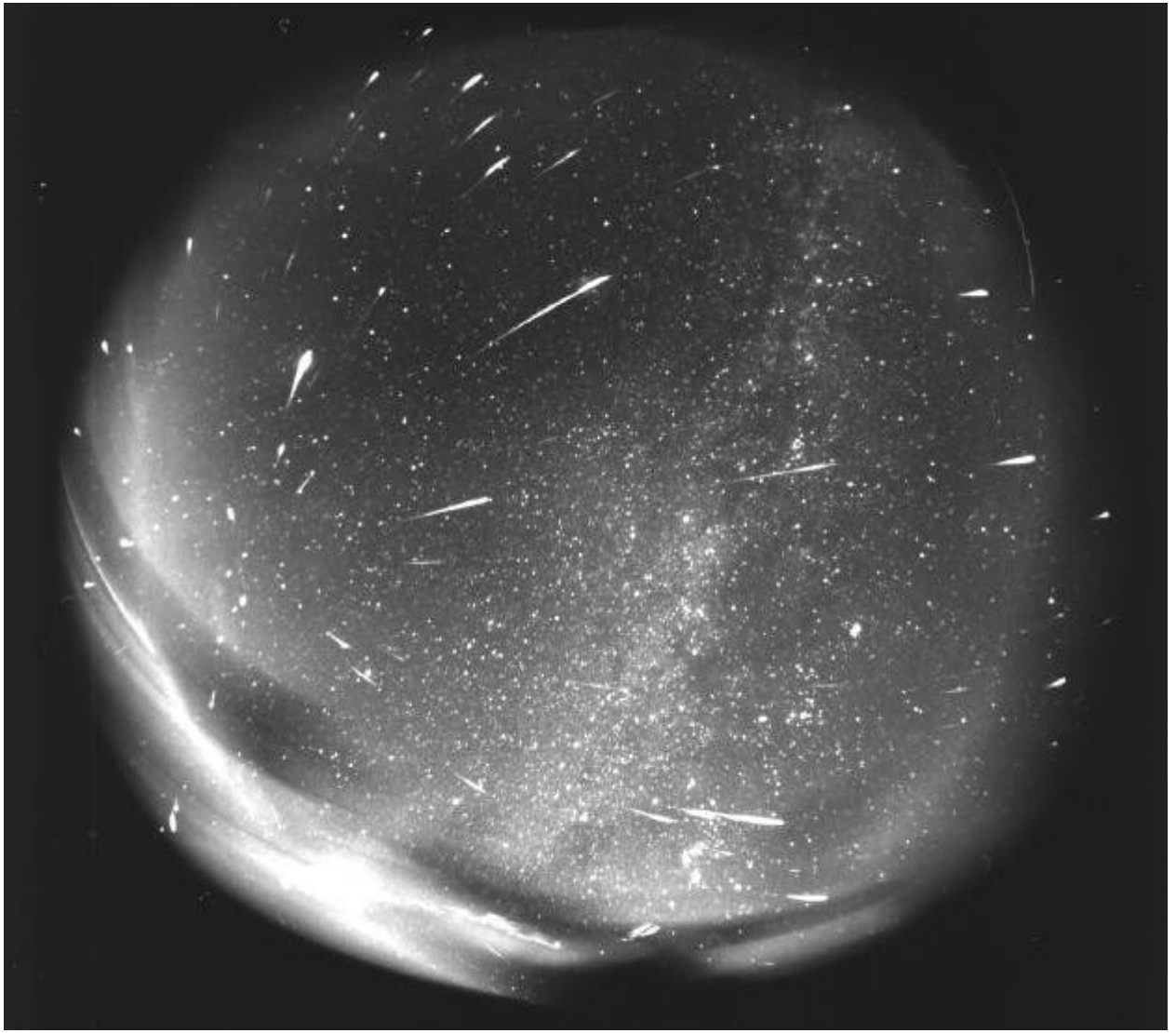

4-urna ekspozicija Leonidov leta 1998 s kamero ribje oko z Observatorija Modra.

Meteorski roji

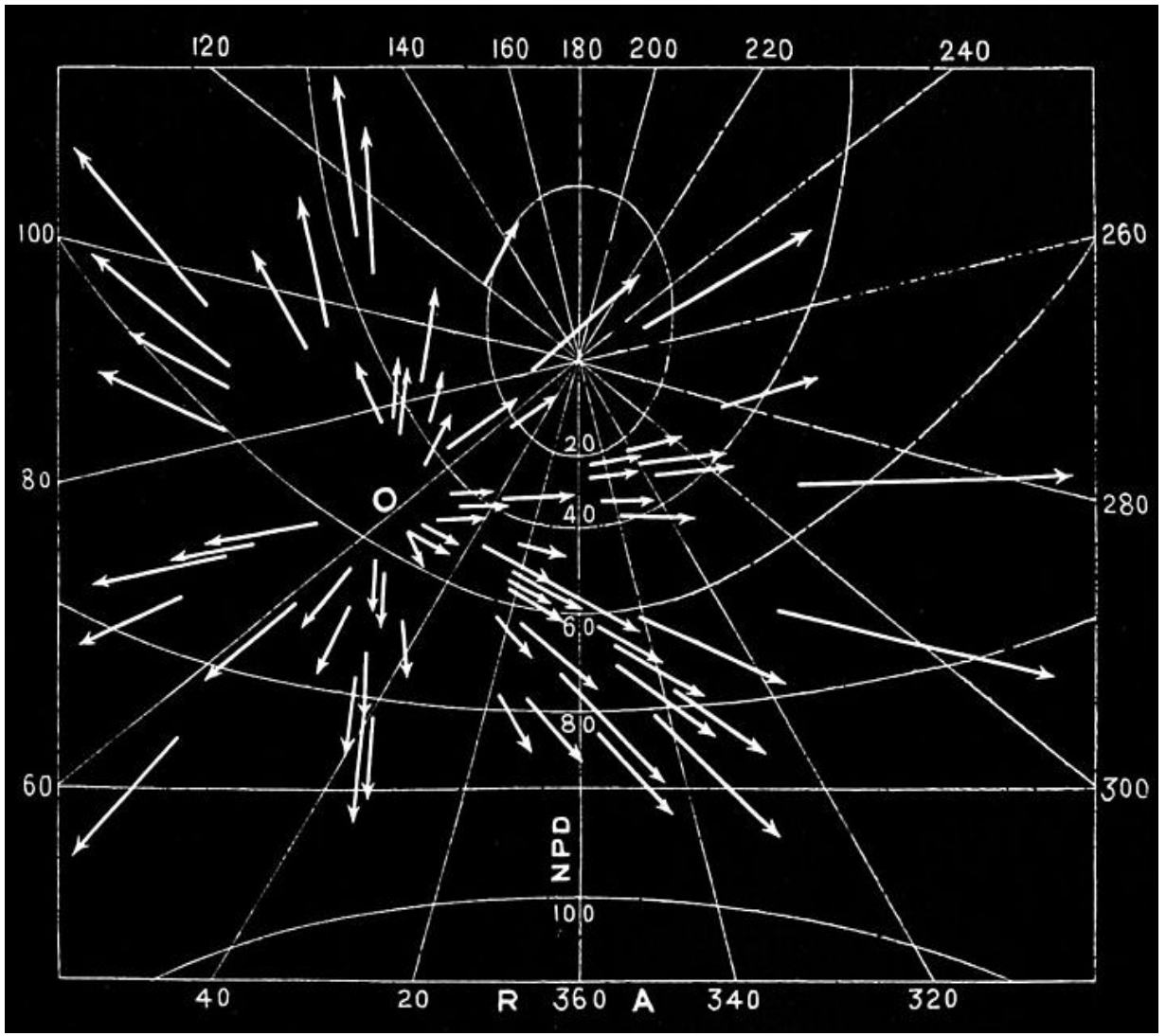

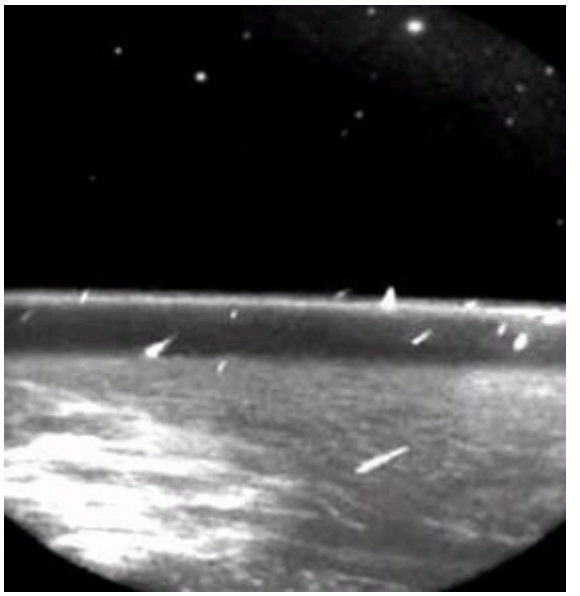

Leonidi iz vesolja.

Beležka Perzeidov na karti iz leta 1880.

Roji nastanejo z (delnim) razpadom kometov. Opazljivi so ~10^4 let.

Shower	Time	Parent object
Quadrantids	Early January	The same as the parent object of minor planet 2003 EH_1,[12] and perhaps comets C/1490 Y1 and C/1385 U1 [13]
Lyrids	late April	Comet Thatcher
Pi Puppids (periodic)	late April	Comet 26P/Grigg-Skjellerup
Eta Aquariids	early May	Comet 1P/Halley
Arietids	mid June	Comet 96P/Machholz, Marsden and Kracht comet groups complex [1][14]
June Bootids (periodic)	late June	Comet 7P/Pons-Winnecke
Southern Delta Aquariids	late July	Comet 96P/Machholz, Marsden and Kracht comet groups complex [1][14]
Alpha Capricornids	late July	Comet 169P/NEAT[15]
Perseids	mid-August	Comet 109P/Swift-Tuttle
Kappa Cygnids	mid-August	Minor planet 2008 ED69[16]
Aurigids (periodic)	early September	Comet C/1911 N1 (Kiess)[17]
Draconids (periodic)	early October	Comet 21P/Giacobini-Zinner
Orionids	late October	Comet 1P/Halley
Southern Taurids	early November	Comet 2P/Encke
Northern Taurids	mid-November	Minor planet 2004 TG_{10} and others [1][18]
Andromedids (periodic)	mid-November	Comet 3D/Biela[19]
Alpha Monocerotids (periodic)	mid-November	unknown [20]
Leonids	mid-November	Comet 55P/Tempel-Tuttle
Phoenicids (periodic)	early-December	Comet D/1819 W1 (Blanpain)[21]
Geminids	mid-December	Minor planet 3200 Phaethon[22]
Ursids	late December	Comet 8P/Tuttle[23]

TABLE 1. Stream orbital and geocentric data.

- epoch B (1950) -

Stream Name	q **(a.u.)**	e	i	ω	Ω	V_G **geocentric velocity (km/s)**	θ	ϕ	Parent **body (all except Phaethon are active comets)**
Leonids	0.98	0.92	162	173	235	71	170	168	55P/Tempel-Tuttle
ε Geminids	0.81	0.96	174	231	203	70	166	258	C/1964N1 Ikeya*
Orionids	0.57	0.97	165	83	29	66	155	288	1P/Halley
Perseids	0.95	0.95	113	150	139	59	139	164	109P/Swift-Tuttle
σ Hydrids	0.24	0.98	126	122	78	58	137	295	
Lyrids	0.92	0.99	80	214	32	47	119	198	C/1861G1 Thatcher
Monocerotids	0.18	1.00	37	129	80	43	112	286	D/1917F1 Mellish
Quadrantids	0.98	0.68	72	171	282	41	116	176	96P/Machholz 1
S. δ Aquarids	0.08	0.97	27	151	308	41	118	278	96P/Machholz 1
N. δ Aquarids	0.10	0.95	21	328	142	38	117	262	96P/Machholz 1
Geminids	0.14	0.90	24	324	261	35	117	258	(3200) Phaethon
α Virginids (S)	0.32	0.87	7	118	198	31	103	275	
Taurids (N)	0.32	0.85	3	299	213	30	104	267	2P/Encke
Taurids (S)	0.34	0.82	6	118	27	28	104	275	2P/Encke
χ Orionids (N)	0.38	0.83	3	291	265	28	101	267	
α Virginids (N)	0.41	0.83	8	288	34	28	99	263	
κ Cygnids	0.98	0.76	39	202	147	25	88	194	
χ Orionids (S)	0.51	0.79	5	96	77	25	93	276	
α Capricornids (N)	0.58	0.78	6	268	134	23	89	262	45P/Honda-Mrkos-Paidušáková
ε Piscids (N)	0.58	0.76	5	268	190	22	89	263	
ε Piscids (S)	0.61	0.73	4	85	5	21	88	276	
α Capricornids (S)	0.63	0.62	4	89	329	18	89	276	45P/Honda-Mrkos-Paidušáková
α Pegasids	0.97	0.68	7	200	230	11	42	226	

* *Olsson-Steel* (1987) found that Comet C/1987B1 Nashikawa-Takamizawa-Tago is as good a candidate to be the parent of the ε Geminids as is C/1964N1 Ikeya (*Drummond,* 1981).

Vir: Jopek T., Valsecchi G.B., Froeschle C.
V geocentričnem sistemu: $\mathbf{V_G}$ = geocentrična hitrost, θ, Φ pa polarna kota ob sekanju Zemljinega tira
θ – kot med smerjo roja in hitrostjo Zemlje ob sekanju Zemljinega tira,
Φ – kot v ravnini pravokotni na hitrostni vektor Zemlje ob sekanju: 0° za gibanje proti severnem ekl. polu, 90° za gibanje v ekliptiki radialno ven, 180° za gibanje proti juznemu ekl. polu, 270° za gibanje v ekliptiki proti Soncu.

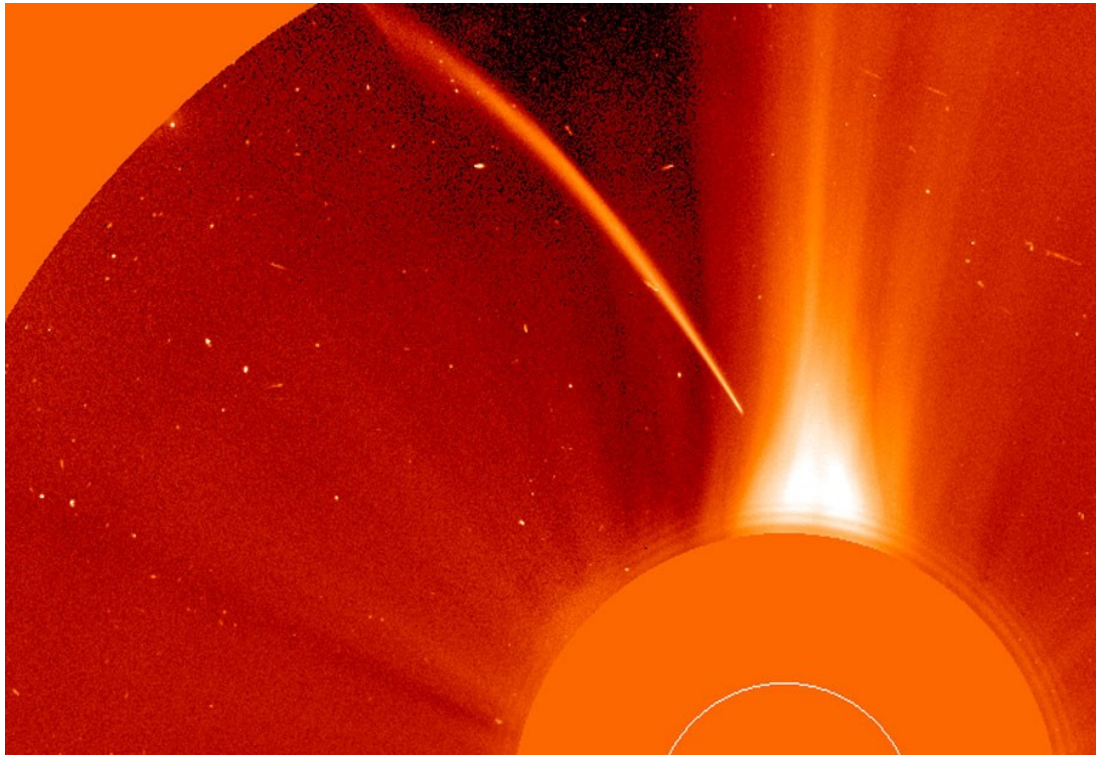

Padec kometa v Sonce

Sungrazer
Credit: LASCO, SOHO Consortium, NRL, ESA, NASA

Explanation: The Sun destroyed this comet. Arcing toward a fiery fate, this Sungrazer comet was recorded by the SOHO spacecraft's Large Angle Spectrometric COronagraph(LASCO) on 1996 Dec. 23. LASCO uses an occulting disk, partially visible at the lower right, to block out the otherwise overwhelming solar disk allowing it to image the inner 5 million miles of the relatively faint corona. The comet is seen as its coma enters the bright equatorial solar wind region (oriented vertically). Spots and blemishes on the image are background stars and camera streaks caused by charged particles. Positioned in space to continuously observe the Sun, SOHO has now been used to discover over 1,500 comets, including numerous sungrazers. Based on their orbits, they are believed to belong to a family of comets created by successive break ups from a single large parent comet which passed very near the Sun in the twelfth century. The Great Comet of 1965, Ikeya-Seki, was also a member of the Sungrazer family, coming within about 650,000 kilometers of the Sun's surface. Passing so close to the Sun, Sungrazers are subjected to destructive tidal forces along with intense solar heat. This comet, known as SOHO 6, did not survive.

Padec kometa v Jupiter

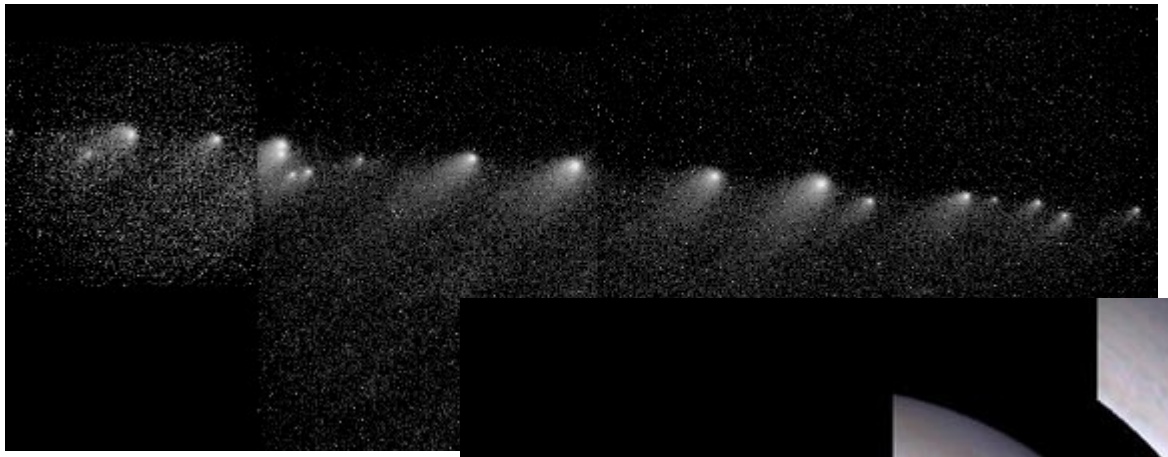

Shoemaker Levy 9 (leta 1994).

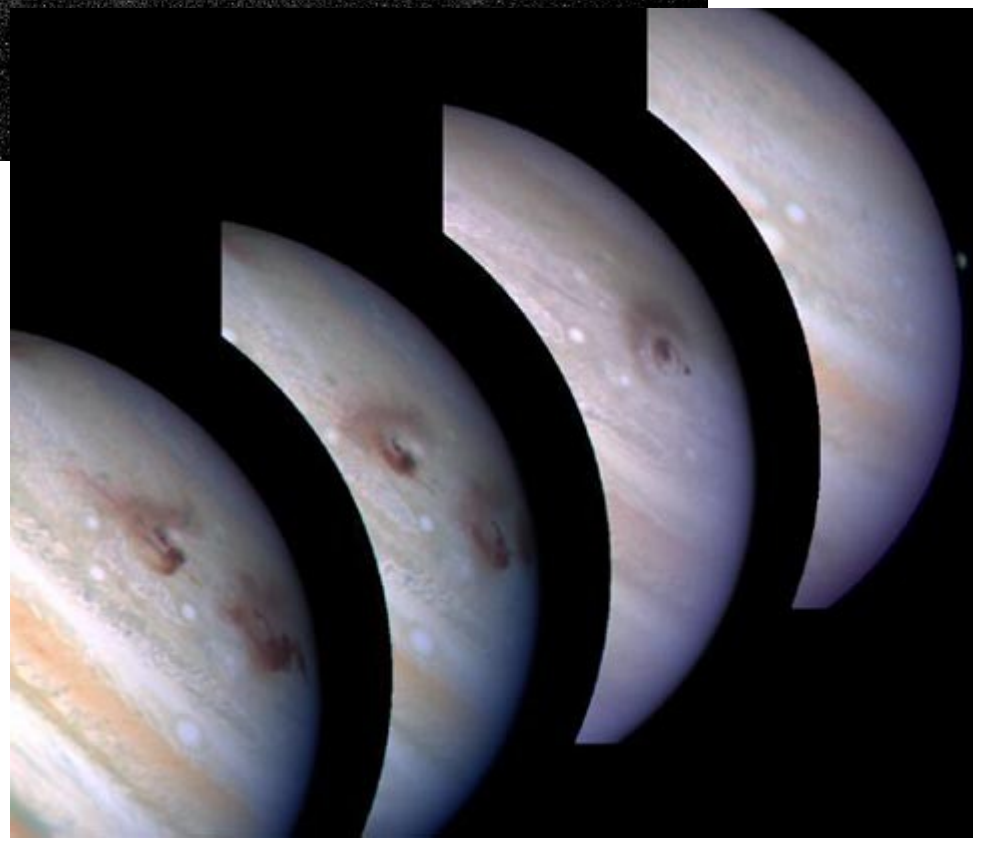

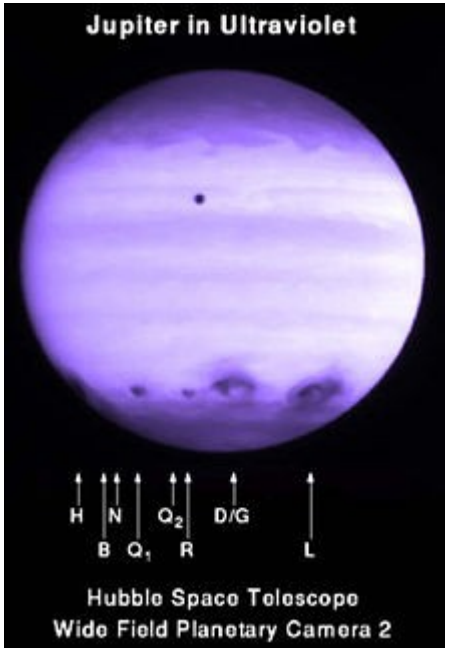

Jupiter v UV svetlobi ~2 uri po padcu fragmenta R.

Veriga kraterjev na luni Ganimed, morda posledica podobnega dogodka.

Afeliji periodičnih kometov

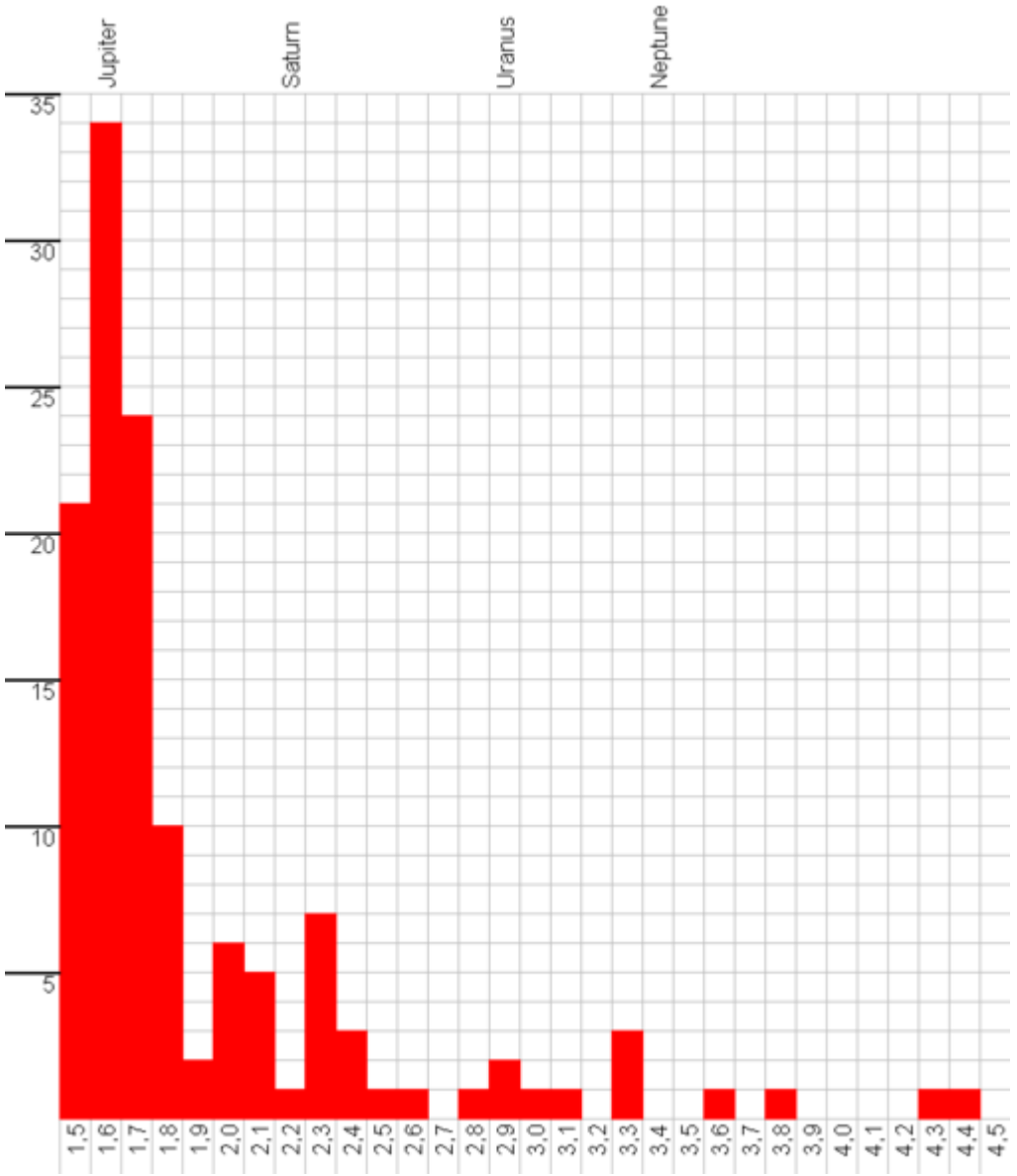

ln(afelij/a.e.)

Prevladuje
Jupitrova družina

Splošna porazdelitev kometnih velikih polosi

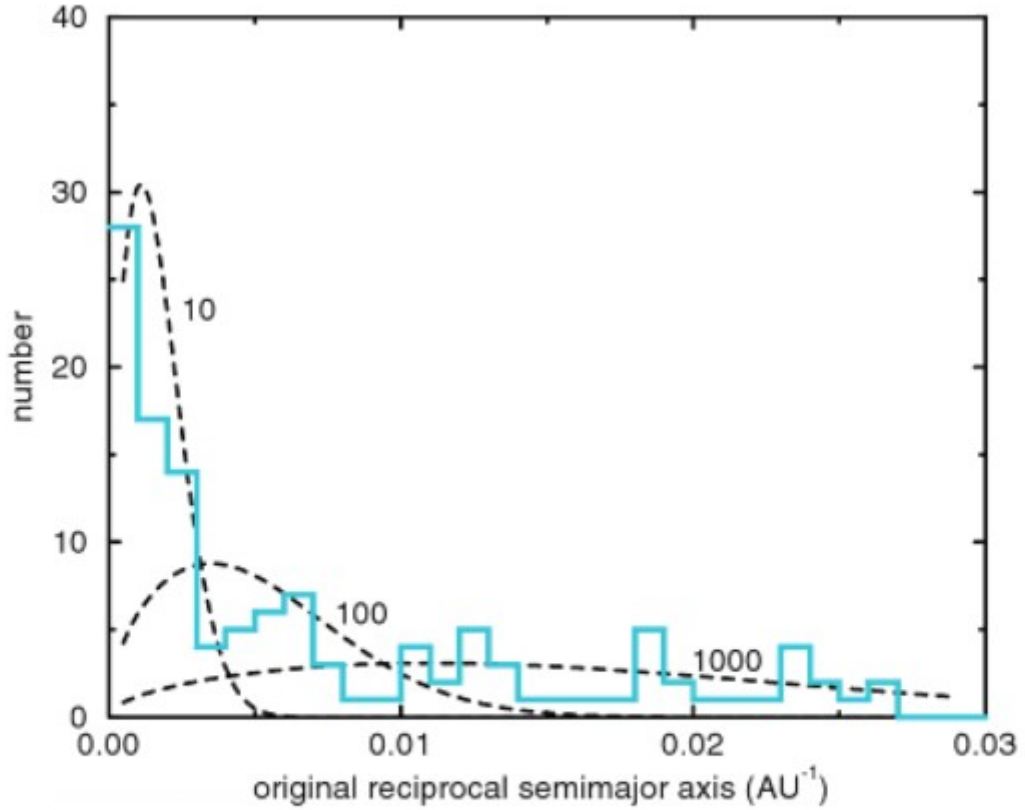

Figure 4.6. Distribution of the original reciprocal semimajor axes of long-period comets with binding energies $x < -10^{-4}$ AU^{-1} (or $a_{orig} < 10^4$ AU) and perihelion distances $q < 1.5$ AU. Three theoretical distribution functions, derived for physical lifetimes of 10, 100 and 1000 revolutions as given by eq. (4.41), are superimposed to the histogram (Fernández and Gallardo 1999).

Vir: Julio A. Fernández: Comets: Nature, Dynamics, Origin, And Their Cosmogonical Relevance

Splošna porazdelitev kometnih naklonov

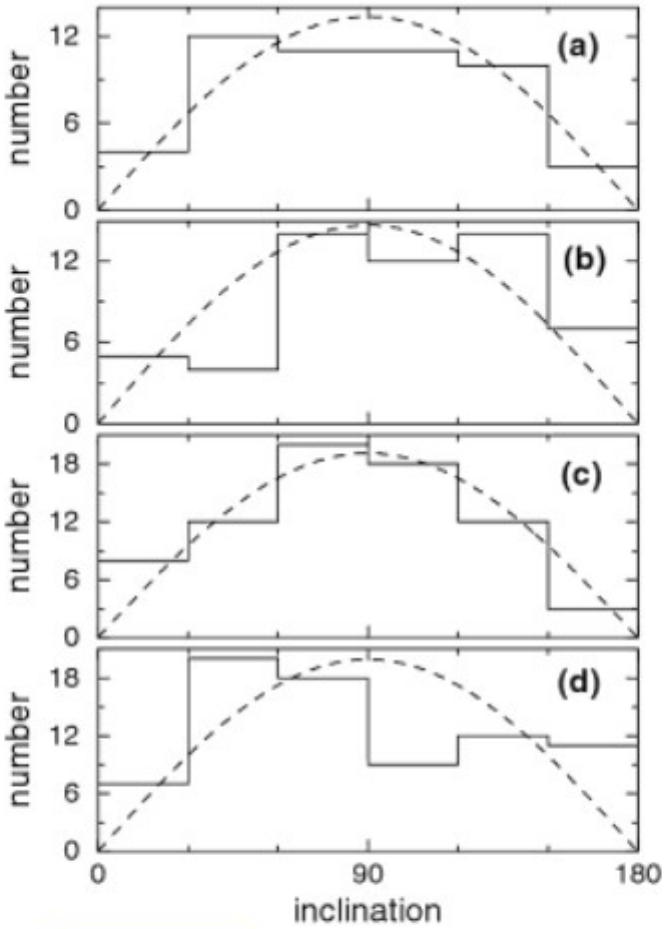

Figure 4.7. Inclination distribution of LP comets with perihelion distances $q < 2.5$ AU for different dynamical states of evolution: (a) "new" ($0 > x > -10^{-4}$ AU^{-1}), (b) "young" ($-10^{-4} > x > -10^{-3}$ AU^{-1}), (c) "middle-age" ($-10^{-3} > x > -5 \times 10^{-3}$ AU^{-1}), and (d) "old" ($-5 \times 10^{-3} > x > -2.92 \times -10^{-2}$ AU^{-1}). A sinusoidal curve has been fitted to each one of the histograms. Data taken from Marsden and Williams (2003) catalogue, leaving aside the families of sungrazers.

Vir: Julio A. Fernández: Comets: Nature, Dynamics, Origin, And Their Cosmogonical Relevance

Kuiperjev pas

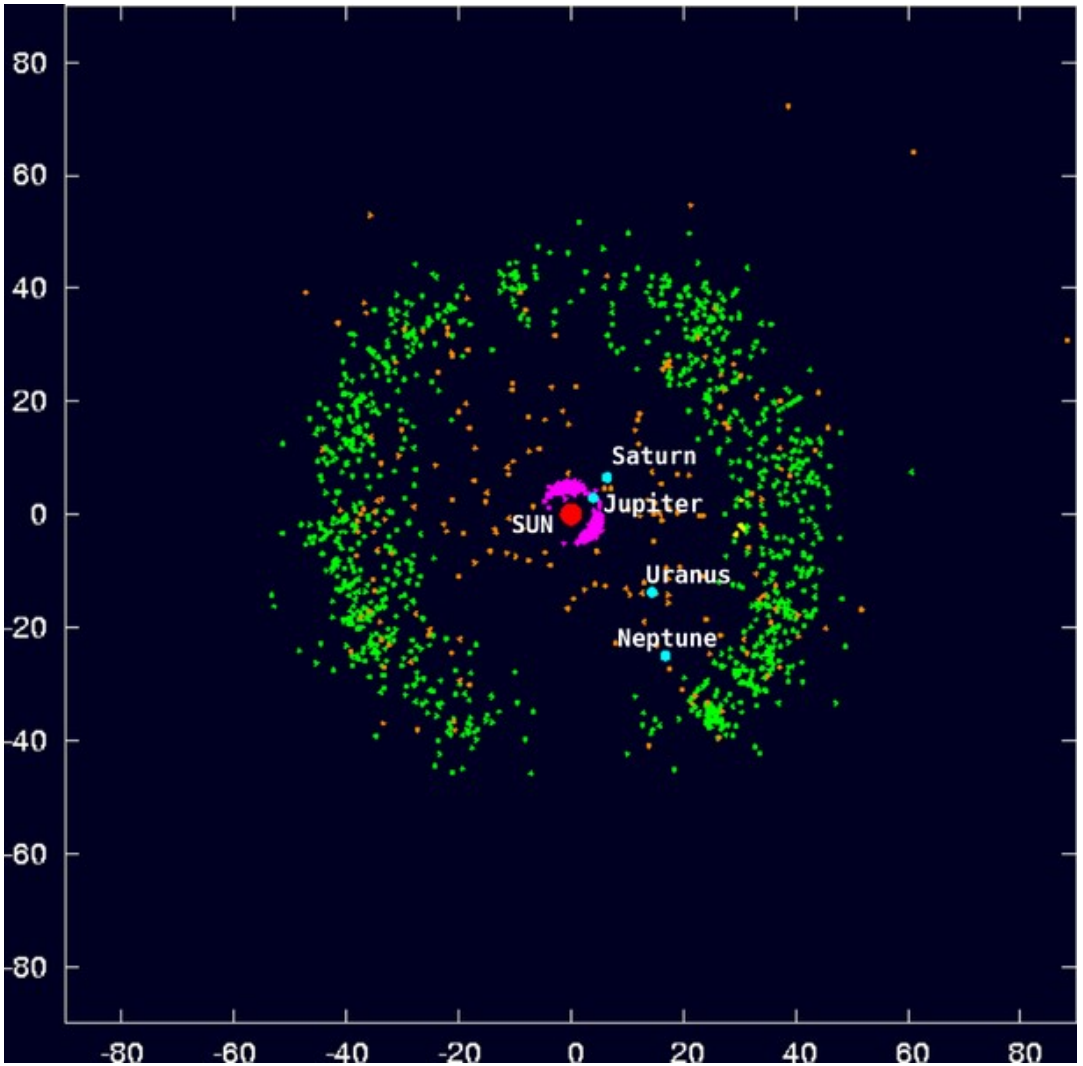

Legend

Red = The Sun
Aquamarine = Giant Planet
Green = Kuiper belt object
Orange = Scattered disc object or Centaur
Pink = Trojan of Jupiter
Yellow = Trojan of Neptune

Axes list distances in AU, projected onto the ecliptic, with ecliptic longitude zero being to the right, along the "x" axis).

Positions are accurate for January 1st, 2000 (J2000 epoch) with some caveats: For planets, positions should be exact. For minor bodies, positions are extrapolated from other epochs assuming purely Keplerian motion. As all data is from an epoch between 1993 and 2007, this should be a reasonable approximation.

Data from the Minor Planet Center[1] or Murray and Dermott[2].

Radial "spokes" of higher density in this image, or gaps in particular directions are due to observational bias (i.e. where objects were searched for), rather than any real physical structure. The pronounced gap at the bottom is due to obscuration by the band of the Milky Way.

Ooortov oblak

As discussed in Chapter 1, at the middle of the last century the debate on whether comets were members of the solar system or interstellar bodies was still unsettled. The main hurdle against an origin in the solar system was to explain how cometary orbits, that presumably shared at the beginning the coplanarity of the planets and asteroids, could have later acquired a random distribution. In 1950 the Dutch astronomer Jan Hendrik Oort (1900-1992) found that the distribution of original reciprocal semimajor axes of the sample of LP comets known at that moment showed a strong excess within the narrow range $0 < (1/a)_{orig} < 10^{-4}$ AU^{-1}. As we discussed before, these are the so-called "new" comets. It is very likely that after a single passage most new comets will be either ejected to interstellar space or transferred to more tightly bound orbits. This finding led Oort (1950) to the conclusion that a huge swarm of $\sim 10^{11}$ comets surrounds the solar system at distances of a few 10^4 AU. This structure, called the *Oort cloud*, is generally supposed to be the source of LP comets. According to Oort, comets originally formed in the planetary region, the asteroid belt being the most likely source region, which was the only substantial population of minor bodies known at that time. He further argued that planetary perturbations were responsible for scattering comets to near interstellar distances where perturbations by passing stars randomized their orbital planes and re-injected some of these comets in the inner planetary region, thus becoming potentially observable. Oort depicted what later became a standard model of the Oort cloud, with the exception of the source region, The asteroid belt does not seem to be a suitable source, basically because of the very different compositions: asteroids are rocky bodies while comets are ice-rich bodies.

Vir: Julio A. Fernández: Comets: Nature, Dynamics, Origin, And Their Cosmogonical Relevance

Ooortov oblak

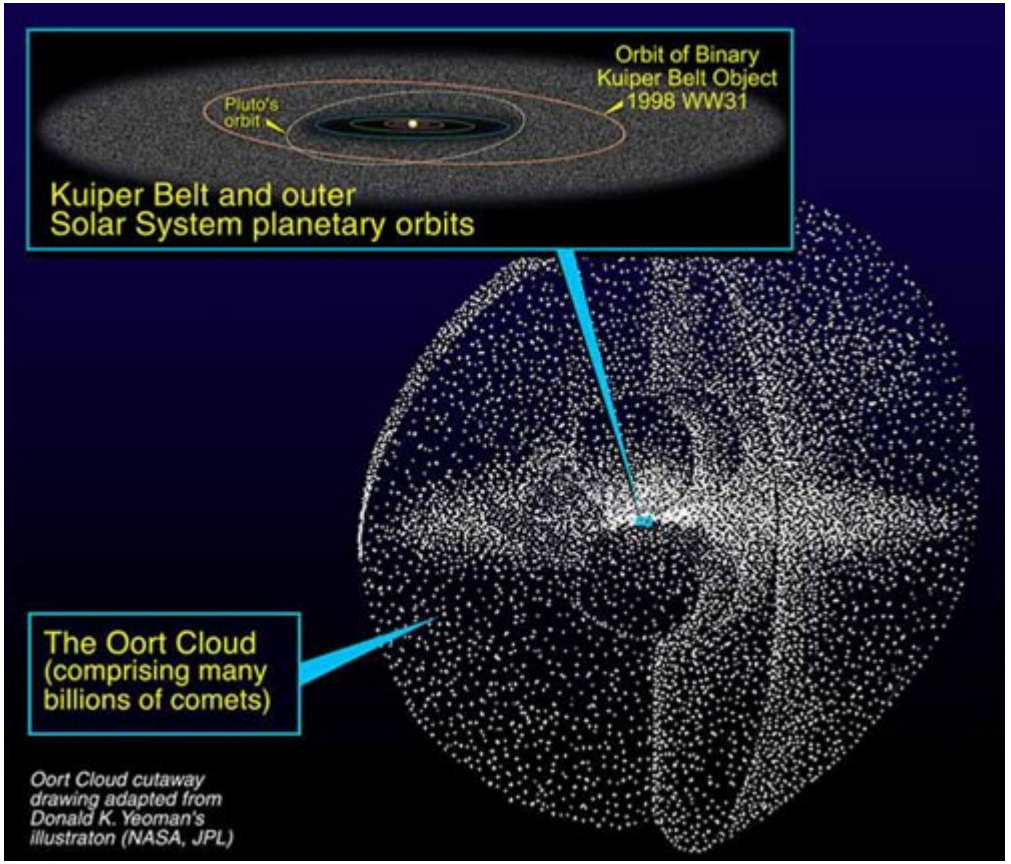

Possible Oort cloud objects

Number	Name	Equatorial diameter (km)	Perihelion (AU)	Aphelion (AU)	Year discovered	Discoverer	Diameter method
90377	Sedna	1,180–1,800 km	76.23	1009	2003	Brown, Trujillo, Rabinowitz	thermal[49]
148209	2000 CR_{105}	~250 km	44.3	397	2000	Lowell Observatory	assumed[50]
308933	2006 SQ_{372}	50–100 km	24.17	2,005.38	2006	SDSS	assumed[51]
–	2008 KV_{42}	58.9 km[52]	20.217	71.760	2008	Canada–France–Hawaii Telescope	assumed[8]

Porazdelitev kometnih perihelijev

The Distribution of the Perihelia of Comets.

GENTLEMEN,—

I am glad that my letter has been the occasion of calling forth the interesting communication from Dr. Holetschek, which appears in No. 152; but there are some points on which I cannot concur with him.

Of course the northern situation of our observing-stations will have more effect in preventing the detection of comets whose perihelia have high southern latitudes than where the southern latitudes of the perihelia are small. Dr. Holetschek's figures (which substantially agree with mine) bring out this clearly. The number of northern and southern perihelia are nearly equal between latitudes 0° and 30°, while from 30° to 90° the northern perihelia preponderate in the ratio of more than 2 to 1. A deficiency of comets whose perihelia have high *southern* latitudes thus arises from the northern situation of our observatories.

Turning, then, to comets with northern perihelia, the question arises whether there is any deficiency of *these* comets at high latitudes. The latitude-circles are of course small circles on the sphere, whose circumferences diminish as the latitude becomes greater. A uniform distribution of perihelia would not therefore give the same number between 30° and 60° latitude as between 0° and 30°, or the same number between 60° and 90° latitude as between 30° and 60°. If I am right, the proportions in these three intervals should (if the distribution was uniform) be as 1000, 732, and 268. The actual proportions for northern aphelia, according Dr. Holetschek's table, are 1000, 738, and 284—the very slight departure from uniformity thus indicating a tendency to high rather than to low latitudes. The conclusion appears to be that, so far as latitude is concerned, the distribution of the perihelia of comets is nearly uniform, but that, owing to the northerly position of our observatories, a large number of comets whose perihelia have high southern latitudes escape observation.

The clustering of aphelia (and of course also of perihelia) about longitudes 90° and 270°, together with the well-marked minima which occur about halfway between these maxima, seem to me rather to indicate a connexion between cometary aphelia and the Galaxy. A degree of longitude includes the largest portion of the Galaxy at the intersections of the Galaxy with the ecliptic and the smallest portion at the points where the Galaxy lies furthest to the north or the south of the ecliptic. The four points thus determined agree very closely with the maxima and minima of cometary perihelia as regards longitude.

Truly yours,

1889, August 15. W. H. S. MONCK.

THE ASTROPHYSICAL JOURNAL, 472:L41–L43, 1996 November 20

TIDAL IMPRINT OF DISTANT GALACTIC MATTER ON THE OORT COMET CLOUD

JOHN MATESE AND DANIEL WHITMIRE
Department of Physics, University of Southwestern Louisiana, Lafayette, LA 70504-4210; matese@usl.edu
Received June 3; accepted September 10

ABSTRACT

We report the detection of a remarkably strong nonrandom signal in the distribution of perihelia vectors of Oort cloud comets. The strongest signal is in the Galactic longitudes of perihelia, and we show that it is most likely caused by the adiabatic perturbation of the Galactic radial tide. The probability that the signal in longitude is because of chance is found to be 2×10^{-6}. There is also evidence of the adiabatic perturbation of the Galactic tide component which is in a direction normal to the midplane. This is found in the distribution of Galactic latitudes of perihelia but is statistically less significant, a somewhat counterintuitive result since the Galactic z tide has a strength $\approx$16 times that of the Galactic radial tide. We find that $\approx$1/3 of observed Oort cloud comets are attributable to the Galactic radial tide. The source of the Galactic z tide is primarily local disk matter, while the source of the Galactic radial tide is the entire distribution of matter interior to the solar orbit. Consequently, we conclude that distant matter in the Galaxy, down to the Galactic core some 1.6×10^9 AU away, is an important factor in making Oort cloud comets observable.

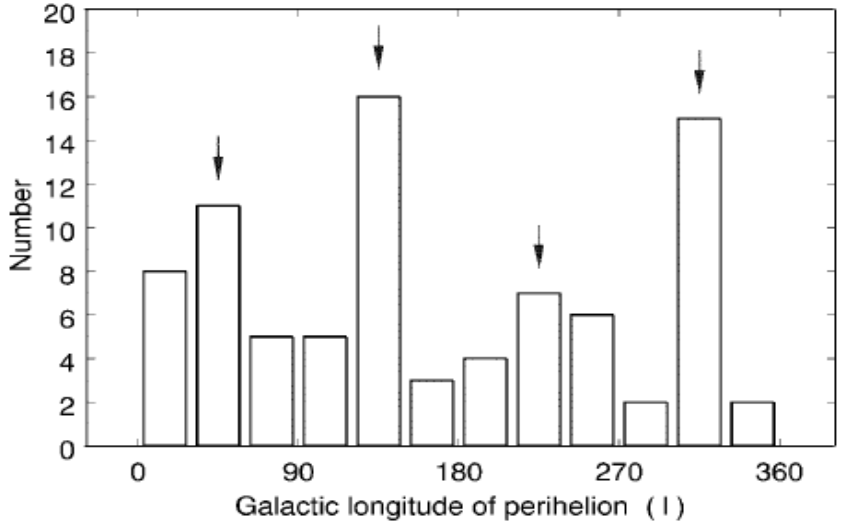

FIG. 2.—Distribution of the longitudes of perihelia in Galactic coordinates for class I Oort cloud comets. A random distribution would be uniform in l. The arrows mark the bisectors of the predicted minima in the distribution when the radial tide is included.

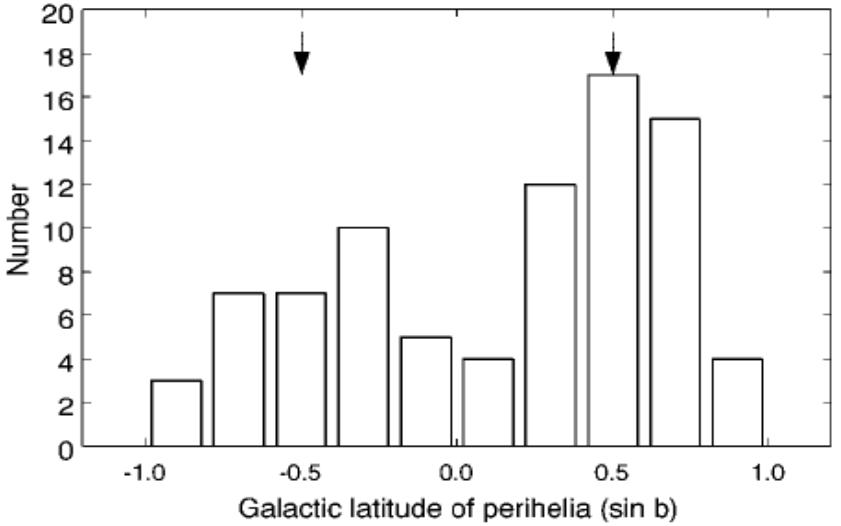

FIG. 3.—Distribution of the latitudes of perihelia in Galactic coordinates for class I Oort cloud comets. A random distribution would be uniform in sin b. The arrows mark the bisectors of the predicted minima in the distribution. The north-south Galactic asymmetry may be caused by historical selection effects resulting from a deficiency of geocentric southern hemisphere observers (Delsemme 1987).

Rickman, H. et al. 2008

Pomembne so tudi motnje mimo letečih zvezd

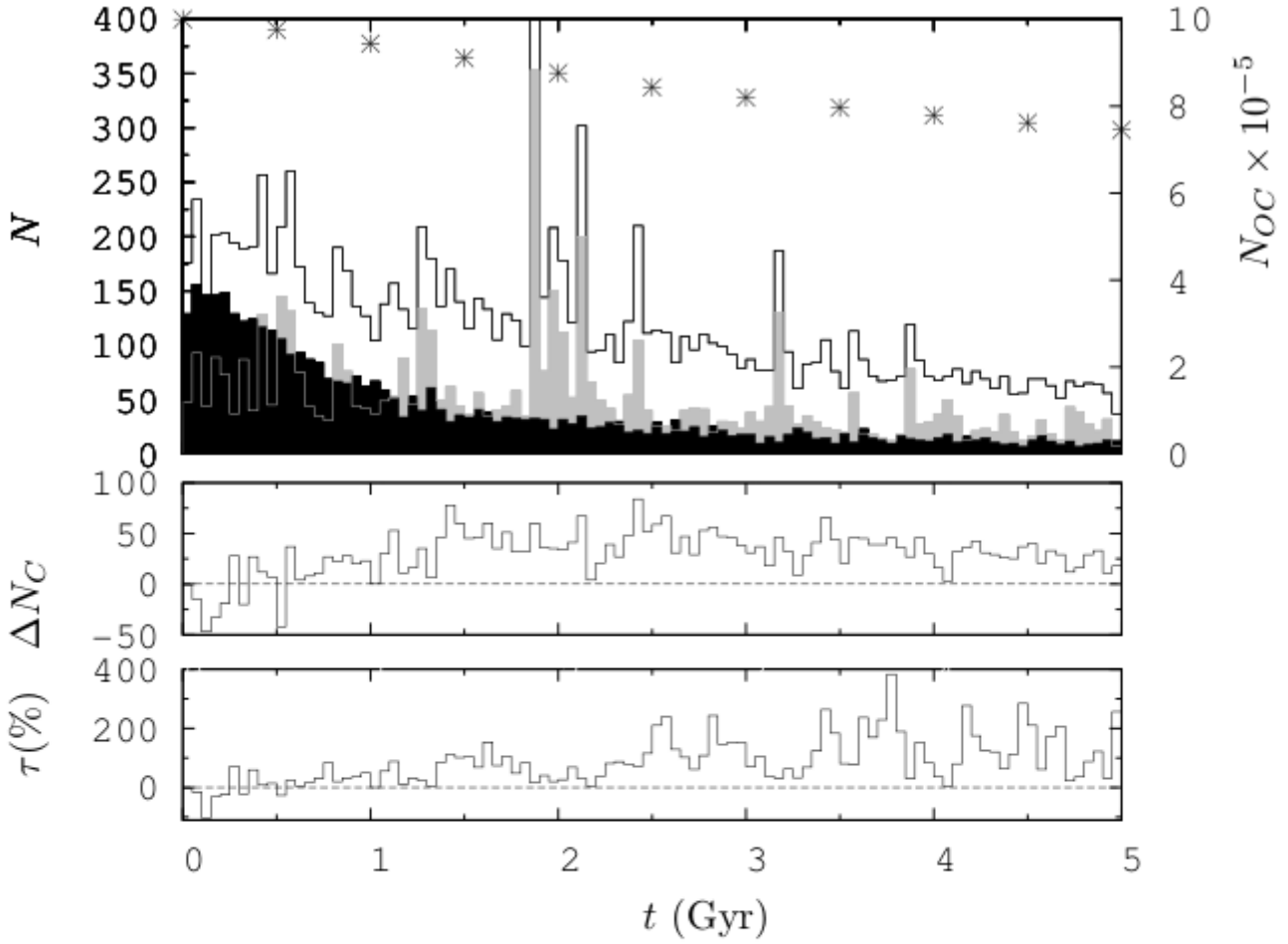

Figure 2. The upper diagram shows the number of comets entering the observable zone per 50 Myr versus time. The white histogram corresponds to the combined model, the black histogram to the Galactic tide alone, and the grey histogram to the passing stars alone. The asterisks indicate the number of comets remaining in our simulation for the combined model at every 500 Myr with scale bars to the right. The middle diagram shows the excess number of injections into the observable region per 50 Myr in the combined model with respect to the sum of the stars-only and tides-only models. The lower diagram shows this excess expressed in percent of the mentioned sum.

Pomembne so tudi motnje mimo letečih zvezd

Rickman, H. et al. 2008

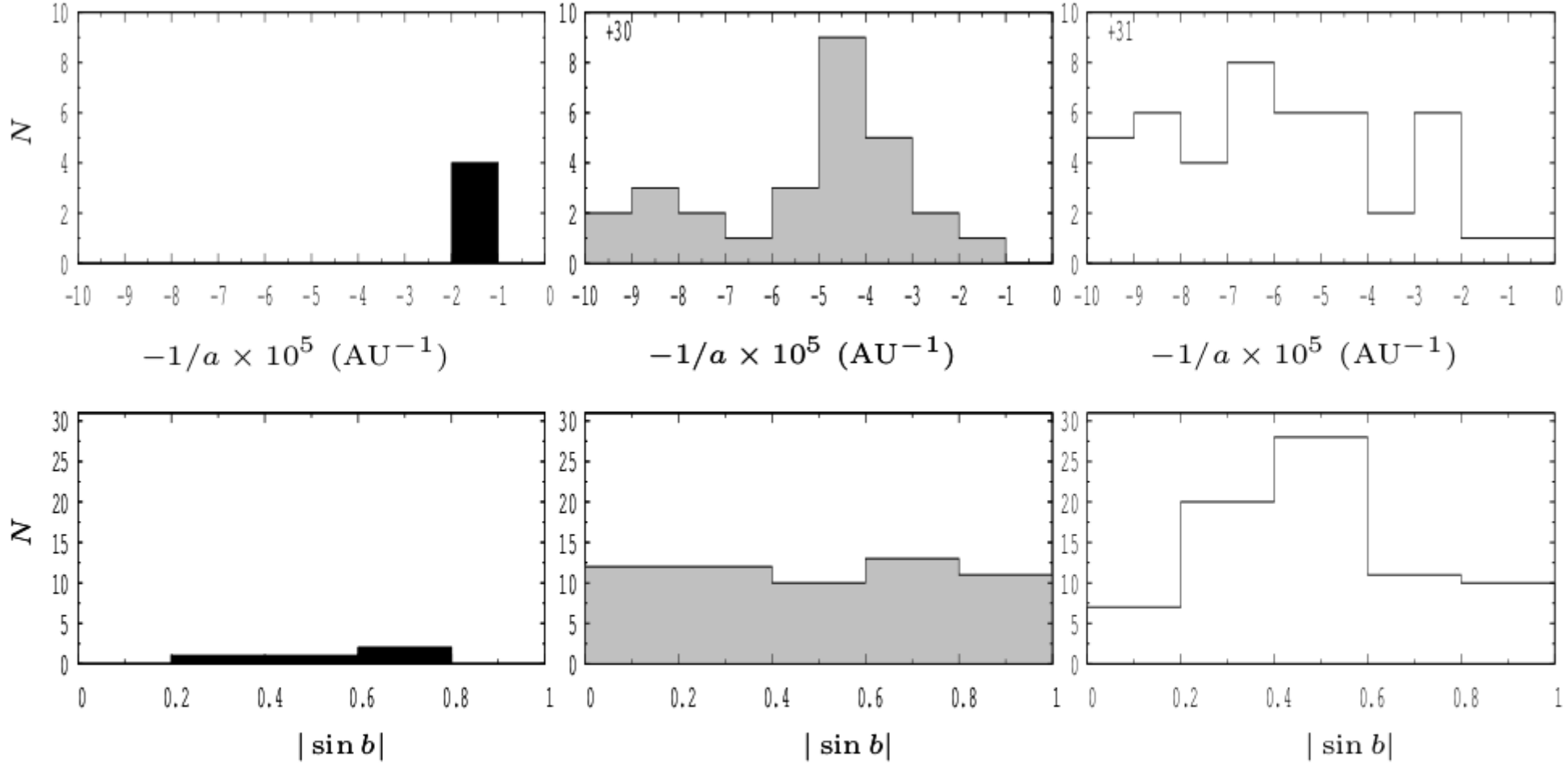

Figure 6. Same as Fig. 5 but considering the comets that enter the observable region during a shower between 3.85 and 3.86 Gyr. The shower is due to a M5 star with impact parameter 2 055 AU, velocity 17.7 km/s and mass 0.21 $M_\odot$.